CONF-760610--1

"Crack Propagation with Crack Tip Critical Bending Moments in DCB Specimens"[+]

by

S. J. Burns and C. L. Chow
Department of Mechanical and Aerospace Sciences,
University of Rochester
Rochester, N. Y. 14627, U. S. A.

[+]This work was supported by the Energy Research and Development Administration.

DISCLAIMER

ABSTRACT

Rapidly wedged, double cantilevered beam specimens have a critical bending moment as a propagating fracture criterion in the limit of Bernoulli-Euler beam theory. The magnitude of the critical bending moment is calculated from a fully dynamic analysis of crack propagation. The shear force, in the beam at the constant displacement rate end of the DCB specimen, multiplied by the square root of the loading time is related to the critical bending moment. Experimental measurements of the time dependence of the shear force have been used to calculate the specific fracture surface energy versus crack velocity. The crack velocity in a single specimen decreases with increasing time, it varies by a factor of 5 and is typically 0.01 of $\sqrt{E/\rho}$. Details of the experimental measurements for brittle and ductile fractures, including stress intensity values versus crack velocity are described.

Key words: double cantilevered beam specimens, rapid crack propagation, fracture, fast fracture, dynamic stress intensity factors, shear force, critical bending moments, crack velocity.

INTRODUCTION

The critical stress intensity factor for a propagating crack, K_{ID}, is a function of the crack velocity, the temperature of the test specimen and the material tested. K_{ID} values in the literature have been measured in double cantilevered beam (DCB) specimens by experimentally observing the crack length as a function of time or the stress intensity factors before and after crack propagation [1,2]. The object of this paper is to report on measurements of K_{ID} obtained by recording the time dependence of the shear force in DCB specimens that have been rapidly wedged open.

All reported K_{ID} values in the literature are found by comparing specific parameters calculated from dynamic mechanics analysis of a propagating crack, with a prescribed specimen geometry and loading [3,4], to experimental measurements of the same parameters. In the rapidly wedged DCB specimen the crack velocity decreases as the crack length increases so measured K_{ID} values are often recorded over an order of magnitude in crack velocities from a single specimen [1].

K_{ID} values in the literature frequently show significant experimental scatter. Part of the experimental scatter is directly affected by the difficulty of absolute measurements of the crack length. In the simple static DCB specimen with a fixed opening at the load end, the specific fracture surface energy, R, depends on the fourth power of the crack length. Thus, a 10% error in the measured crack length gives a 40% error in R. The approach used in this paper is to experimentally apply a constant rate opening on the end of the DCB specimen and experimentally measure the shear force near the load end as a function of time. The R values during

crack propagation are computed from the time dependence of the shear force as calculated from the dynamic mechanics analysis of the rapidly wedged DCB specimen [3]. For plane strain fracture $R = \frac{K_{ID}^2}{E}(1-\nu^2)$ when the crack speeds are slower than several % of the sound speed, however if crack speed is very large then K_{ID} is not simply related to the measured R value. In an infinite solid the analysis of Broberg [5] or Freund [6] relates R to K_{ID}.

The fracture criterion in DCB specimens in the limit of Bernoulli-Euler beam theory, with the beam built-in at the crack tip is a critical bending moment, M*, at the crack tip. In general, the value of M* may depend on the crack velocity, $\dot{\ell}$.

$$M^* = (R(\dot{\ell})WEI)^{\frac{1}{2}} \qquad (1)$$

where W is the width of the crack, E is Young's modulus and I is the moment of inertia of one arm of the beam about the neutral axis. This paper describes in detail how the critical bending moment and thus $R(\dot{\ell})$ may be deduced during crack propagation. In static beam theory the bending moment at the crack tip is given by the shear force at the load end times the crack length.

In rapidly wedged, dynamic crack propagation the value of the bending moment is determined by the shear force times the square root of the time subsequent to the contact of the wedge with the specimen.

The Procedure Section formally relates the shear force to the specific fracture surface energy. Also included are the shear force measurement techniques. The Experimental Results Section describes the experimental measurements on rapidly wedged DCB specimens and the interpretation of these measurements. K_{ID} versus crack velocity data is also presented in this section. In the Conclusion Section the general findings are summarized.

PROCEDURE

Relating the Shear Force to the Specific Fracture Surface Energy

The analytic solution for crack propagation in rapidly wedged DCB specimens is found in reference [3]; the solution is restricted to slender Bernoulli-Euler beam theory with constant specific fracture surface energy. The beam is considered built-in at the crack tip. The initial condition, during rapid wedging, is zero crack length at zero time. The displacement of the neutral axis of the beam, $y(x,t)$ is also given in the analytic solution [3]. In $y(x,t)$, x is the distance from the load end of the beam to a point along the beam; t is the time subsequent to the contact of the wedge with the beam. The shear force in the beam, $Q(x,t)$ is computed from the third derivative of $y(x,t)$ by

$$EI \frac{\partial^3 y}{\partial x^3}(x,t) = Q(x,t) \tag{2}$$

A dimensionless shear quantity is formed from $Q(x,t)$.

$$\frac{Q(x,t)\sqrt{t}}{(EI)^{\frac{1}{4}}(\rho A)^{\frac{3}{4}}V_e} \equiv Q_N(x,t)\sqrt{t} \tag{3}$$

where ρ is the density of the beam, A is the cross sectional area of the beam and V_e is the constant end loading velocity of the beam. It is now noted that $Q_N(x,t)\sqrt{t}$ for $x = 0$ is only a function of R, the beam geometry, modulus and density. $Q_N(0,t)\sqrt{t}$ will be given as a function of a dimensionless crack propagation parameter, η_ℓ, where

$$\eta_\ell \equiv \frac{1}{4}\left(\frac{\rho A}{EI}\right)^{\frac{1}{2}} \frac{(\ell(t))^2}{t} \tag{4}$$

$\ell(t)$ is the crack length at the time t. It should be noted that when the time

for the DCB specimen to completely break is known, and when the final crack length is known, then η_ℓ is known for that time. It follows from equation (4) that when η_ℓ = constant, the crack velocity, $\dot{\ell} = \frac{\ell(t)}{2t} \propto \frac{1}{\ell}$. Now, Figure 1 is $Q_N(0,t)\sqrt{t}$ plotted versus η_ℓ as calculated from reference [3]. Figure 2 relates R to η_ℓ during crack propagation. In this second figure R is given in the dimensionless parameter $1/V_e\left(\frac{RW}{\rho A}\right)^{\frac{1}{2}}$. Figure 2 follows directly from reference [3].

The specific fracture surface energy, R, during crack propagation is calculated from experimental data by measuring the shear force at x = 0 as a function of time in the DCB specimen. From this data $Q\sqrt{t}$ is formulated. Note that ideally $Q\sqrt{t}$ and thus $Q_N\sqrt{t}$ is a constant when R is constant. Figure 1 relates the constant value of $Q_N(0,t)\sqrt{t}$ to the constant value of η_ℓ. R during the crack propagation is found from figure (2) since η_ℓ is known.

One benefit of measuring the shear force to obtain the critical stress intensity factor during crack propagation, K_D, is that in the slow crack propagation limit K_D is proportional to $(Q_N\sqrt{t})^{\frac{2}{3}}$. Thus, the error in measurement of Q to 5% and t to 1% should give K_D accurate to 4%. In principle, a shear force measurement gives a more accurate determination of K_D than the direct measurements of the crack length. A second advantage to measuring R from $Q\sqrt{t}$ during crack propagation is that zero time, i.e. when the wedge first contacts the specimen, is determined with reasonable accuracy. This follows immediately since Q(0,t) rises very rapidly when the wedge first contacts the specimen. A simple extrapolation of Q(0,t) to zero shear force determines zero time.

A third benefit to this method of measuring R during crack propagation is that the electronic hardware for measuring the shear force versus time

is the same as that used in the ASTM, K_{Id} programs [7]. Although the interpretation of the data is quite different.

The formal theory of [3] restricts $Q_N(0,t)\sqrt{t}$, η_ℓ and R to be exactly constant during crack propagation. However, it has been shown by comparing static and quasi-dynamic solutions of rapidly wedged DCB specimens, that are not restricted to R = constant, that for $\eta_\ell < 1$ that R may depend on $\dot{\ell}$ during crack propagation [3]. With this restriction on η_ℓ, $Q_N(0,t)\sqrt{t}$ may also depend on t during crack propagation.

Experimental Measurements of the Shear Force

Details of the rapid wedge loading machine and the design of the specimens have been reported elsewhere [8,9]. The wedge loading machine is designed to give rigid loading of the DCB specimen with a constant applied deflection rate. This is achieved by a massive, 300 kg, hammer free falling approximately two meters. The side grooved specimen is typically 7.0 x 2.5 x 40 cm. It is designed to be a slender beam that remains essentially elastic during the fracture test.

The shear force is measured on the DCB specimen by recording the shear strain on the neutral axis of the beam with a 90° rosette strain gage. The 90° rosette gage is placed so it is primarily sensitive to shear forces in the beam and insensitive to axial forces. The gage is located near the load end of the DCB specimen. The gage is placed as near to the neutral axis as possible and approximatley a distance equal to 1/2 the height of the beam away from the load point. Thus, the gage is midway between the load point and the initial crack length in the DCB specimen. The signal from the gage is recorded using a vertical amplifier, plug-in unit on an oscilloscope.

The nominal rise-time of the electronic system is 60 μseconds with a frequency response of 6 kHz. The shear force measurement versus time is recorded photographically using a triggered single sweep of the oscilloscope.

Absolute values of the deflection on the oscilloscope are calibrated to shear force values by statically loading the specimen with a negative shear force as measured with a load cell on a tensile machine. The gage output must be linear in the shear force. The response of the gage has been checked to be linear in the shear force although the slope of the response curve depends partially on the loading arrangement. If the gage were to measure the strain at a point (as opposed to a finite area) on the neutral axis of a beam very far from the load point the gage response should be insensitive to the loading arrangement. For the loading arrangement used during our crack propagation tests the load point is only one beam height away from the gage. So that the detail geometry of the contact of the wedge to the beam can give differences as large as 20% between the calibrated static force and the dynamically measured shear force. It is also important to have the wedge contact the DCB specimen in the mid-plane. A very thin piece of shim-stock between the wedge and DCB specimen is ideal for this purpose. The shear force testing of rapidly wedged DCB specimens is self-calibrating (as will be discussed in the next section).

The photographic record of the shear force versus time during the fracture of a sample, is processed by electronically digitizing the Q trace and replotting $Q\sqrt{t}$ versus t.

EXPERIMENTAL RESULTS

$Q_N\sqrt{t}$ versus t in Ti Alloy

The theory for determining R during crack propagation and the experimental procedures for recording the shear force, Q, during crack propagation were outlined in the previous section. Figure 3 shows Q versus t for a sample of Ti-6Al-4V fractured at room temperature. This material has been investigated for dynamic fracture using direct measurements of crack length versus time [9]. Figure 3 shows several characteristic features of a Q versus t curve for rapidly wedged DCB specimens. The value of Q is zero prior to the wedge contacting the specimen on the left of the figure. The shear force then rises very rapidly after the wedge contacts the specimen. Q at the end of the loading curve reaches a maximum value and then Q descreases with time. The start of crack propagation is identified with the maximum value of Q on the far left of Figure 3. This point corresponds to the intersection of the nearly smooth rising Q versus t curve and the decreasing part of the Q versus t curve after crack propagation. The Q trace is not smooth but shows small amplitude oscillations. At much later times, on the right of figure 3 the value of the shear force first rises rapidly and then decreases very rapidly to zero. Although not shown in figure 3 at longer times the shear force continues to oscillate about the zero value with several mixed frequencies. At very long times a single frequency is achieved and the amplitude of the signal decays as time increases.

The time when the wedge first fully contacted the specimen is determined from the intersection of the zero Q value and the extrapolated intersection of the rapidly rising shear force curve on the left of figure 3. Having defined zero time, $Q\sqrt{t}$ is now formed. $Q\sqrt{t}$ is the information necessary to determine

R during the crack propagation. Figure 4 is $Q_N\sqrt{t}$ versus t for this specimen as computed from the digitized trace of figure 3 with the scale of the ordinate as determined below. $Q\sqrt{t}$ is proportional to $Q_N\sqrt{t}$, where $Q_N\sqrt{t}$ is dimensionless as given in equation (3). On the far right of figure 4 just before $Q\sqrt{t}$ increases rapidly the sample is completely fractured. At this point the crack length is the complete length of the sample and the time for the crack to propagate to this length is known from the abscissa value of t in either the Q or the $Q\sqrt{t}$ curves. Thus, at the end of the fracture n_ℓ is known from the final crack length. At the end of the test $Q_N\sqrt{t}$ may now be determined from figure 1 since n_ℓ is known for the final crack length. The scale of the ordinate axis in figure 4 is now determined. $Q_N(t)\sqrt{t}$ and $n_\ell(t)$ are determined throughout the entire test once the scale of the ordinate is chosen. As the crack approaches the entire length of the test piece, simple beam theory is not strictly applicable, thus the final calibration point may introduce a systematic error of up to 5% in the absolute scale of the $Q_N(t)\sqrt{t}$ trace. It should be noted however that the relative trends in K_D versus crack velocity curves are uneffected by minor adjustments in the scale of the $Q_N\sqrt{t}$ versus t curve. It probably would be more appropriate to calculate the scale of $Q_N\sqrt{t}$ curve by using a crack propagation gage near the mid-point of the DCB specimen.

It should be noted in figure 4 that $Q_N\sqrt{t}$ rises rapidly to a nearly constant value and then oscillates with a period that increases slightly with time. On the extreme right of figure 4, $Q_N\sqrt{t}$ rises very rapidly and then goes to zero. It ultimately would become negative since Q becomes negative. The oscillations during crack propagation in $Q_N\sqrt{t}$ are nearly periodic and are thus believed to be associated with vibrations in the

sample. The surface of the fractured sample showed no indications that the crack hesitated nor deviated from the fracture plane. In the analysis of the $Q_N\sqrt{t}$ data these oscillations will be considered not to contribute to the crack tip bending moment and will be smoothed over in calculating the R data.

If the oscillations in figure 4 are not smoothed then the K_D values, when compared to the smoothed K_D values, throughout the fracture test does not vary by more than ± 5%. However, if the oscillations were interpreted as a rapid variation in η_ℓ during an oscillation of $Q_N\sqrt{t}$ then the crack length would decrease and the crack velocity would be negative between oscillations. This is an unrealistic interpretation whereas vibrational modes in the DCB sample are undoubtly excited during the massive wedge impact. Thus, it is argued that the oscillations in $Q_N\sqrt{t}$ which are approximately of the same period as the free vibration of the beam, do not directly contribute to the crack tip bending moment nor do they represent periodic oscillations of the crack velocity. Thus, for the computation of K_D versus $\dot{\ell}$ as shown in Figure 5 these oscillations have been removed and $\dot{\ell}$ is a smoothed crack velocity.

The K_D values of figure 5 have been corrected for the strain energy beyond the crack tip, i.e. from slender to thick beam specimens. This is an important correction when the crack length is short and comparable to the beam height [10]. The K_D values recorded in figure 5 are about 50% larger than K_{IC} in this material [9]. The fracture mode along the entire sample is by ductile void coalescence. A plane strain fracture condition is not achieved since the fracture surface is not flat. In addition, the calculated, static, plane strain width as obtained from the dynamic K_D value and the static yield value is 50% larger than the measured fracture width.

$Q_N\sqrt{t}$ versus t in Steel

Figure 6 is Q versus t for a 1018 cold rolled steel specimen. The sample was fractured at -196°C. Q rises rapidly on the left of the figure and then decreases with time. On the right of the figure, Q increases and then goes to zero. Q then oscillates about zero with several frequencies. Figure 7 is $Q_N\sqrt{t}$ versus digitized from figure 6 following the same procedure used in figure 4. After rising rapidly during loading $Q_N\sqrt{t}$ varies slowly with time with small amplitude oscillations. Just before the large peak on the right of figure 7, the crack has completely broken the sample. The time value just prior to this peak and the complete length of the broken DCB specimen and therefore the crack, is used to calculate η_ℓ at this point. Figure 1 is now used to determine the scale of the $Q_N\sqrt{t}$ ordinate. The data in Figure 7 is smoothed and K_{ID} versus $\dot{\ell}$ is computed from the smoothed curve. This is shown in Figure 8. The fracture mode of this sample is brittle cleavage and the fracture surface is very flat across the sample. Plane strain fracture values have probably been achieved. In addition to the flat fracture there is only a very small shear lip and the width of the fracture is well in excess of $2.5(K_{ID}/\sigma_y)^2$ where σ_y is the static yield stress.

CONCLUSIONS

The measured shear force in the rapidly wedged DCB specimen when multiplied by the square root of the time is a slowly varying function of time. Acoustic waves on the experimental data are small in amplitude but should be smoothed in analyzing $Q_N\sqrt{t}$. The determination of zero on the time axis is deduced from the shear force versus time curve. The crack velocities typically obtained using this test are a factor of 2 slower than the crack velocities in crack arrest specimens. In a single test the crack velocity varies by a factor of 5 and is typically 0.01 of $\sqrt{E/\rho}$ for the specimens and wedging machine used. The testing scheme has two self-consistency checks; first, the absolute shear force calibration obtained by loading the specimen in a tensile machine should be in reasonable agreement with the shear force calibrated from the end of the fracture test. Second, the initial crack length calculated from the extreme left side of the $Q_N\sqrt{t}$ curve should agree with the measured initial crack length in the actual DCB specimen. The stress intensity data during crack propagation as deduced from the $Q_N\sqrt{t}$ curve shows that the thick to slender beam correction is important for short crack lengths.

K_D data versus crack velocity in Ti-6Al-4V shows little rate dependence over the range of velocities tested. The K_D values obtained from the $Q_N\sqrt{t}$ data is however larger than K_{IC} in this material but smaller than the K as calculated from the energy lost in a Charpy specimen and K as calculated from the load deflection energy in completing the fracture of a K_{IC} test specimen [9]. The K_{ID} data versus crack velocity for the steel specimens however do show a rate dependence -- the faster crack velocities have smaller K_{ID} values. In the range of crack velocities tested, the

rate dependence is not a strong effect and is just larger than the estimated experimental scatter.

ACKNOWLEDGEMENTS

The authors are grateful for support for the development of this fracture test by the Energy Research and Development Administration through contract E(11-1)-2422.

REFERENCES

1]. Burns, S. J. and Bilek, Z. J., Metallurgical Transactions, Vol. 4, 1973, p. 975.

2]. Hahn, G. T., Hoagland, R. G., Kanninen, M. F., and Rosenfield, A. R., Dynamic Crack Propagation, G. C. Sih, ed., Noordhoff, 1973, p. 649.

3]. Bilek, Z. J. and Burns, S. J., Journal of Mech. Phys. Solids, Vol. 22, 1974, p. 85.

4]. Kanninen, M. F., International Journal of Fracture, Vol. 10, 1974, p. 415.

5]. Broberg, K. B., Arkio Fysik, Vol. 18, 1961, p. 159.

6]. Freund, L. B., Journal of Mech. Phys. Solids, Vol. 20, 1972, p. 141.

7]. ASTM, E-24 Committee, Task Force .03.

8]. Burns, S. J., Proceedings of 12th Annual Meeting of Society of Engineering Science, 1975, p. 121.

9]. Burns, S. J., Crack Arrest in Titanium, Air Force Materials Laboratory Technical Report AFML-TR-75-101, July 1975.

10]. Kanninen, M. F., International Journal of Fracture, Vol. 9, 1973, p. 83.

FIGURE CAPTIONS

Figure 1. The analytic relation between $Q_N\sqrt{t}$ and η_ℓ is shown.

Figure 2. The analytic relations between $1/V_e\left(\frac{RW}{\rho A}\right)^{\frac{1}{2}}$ and η_ℓ is shown.

Figure 3. An experimental measurement of Q versus t for a Ti alloy specimen fractured at room temperature. The scale of the ordinate is determined from the final fracture point in Figure 4 (see text).

Figure 4. The experimental values of $Q_N\sqrt{t}$ versus t computed from the data in figure 3. The scale of the ordinate is defined from the final crack length.

Figure 5. K_D versus crack velocity for Ti alloy as calculated from figure 4.

Figure 6. A photographic record of Q versus t for 1018 cold rolled steel fractured at -196°C. The abscissa time axis is 2 msec per division.

Figure 7. The experimental values of $Q_N\sqrt{t}$ versus t computed from the data in figure 6. The scale of the ordinate is defined from the final crack length.

Figure 8. K_{ID} versus crack velocity for 1018 cold rolled steel fractured at -196°C as calculated from figure 7.

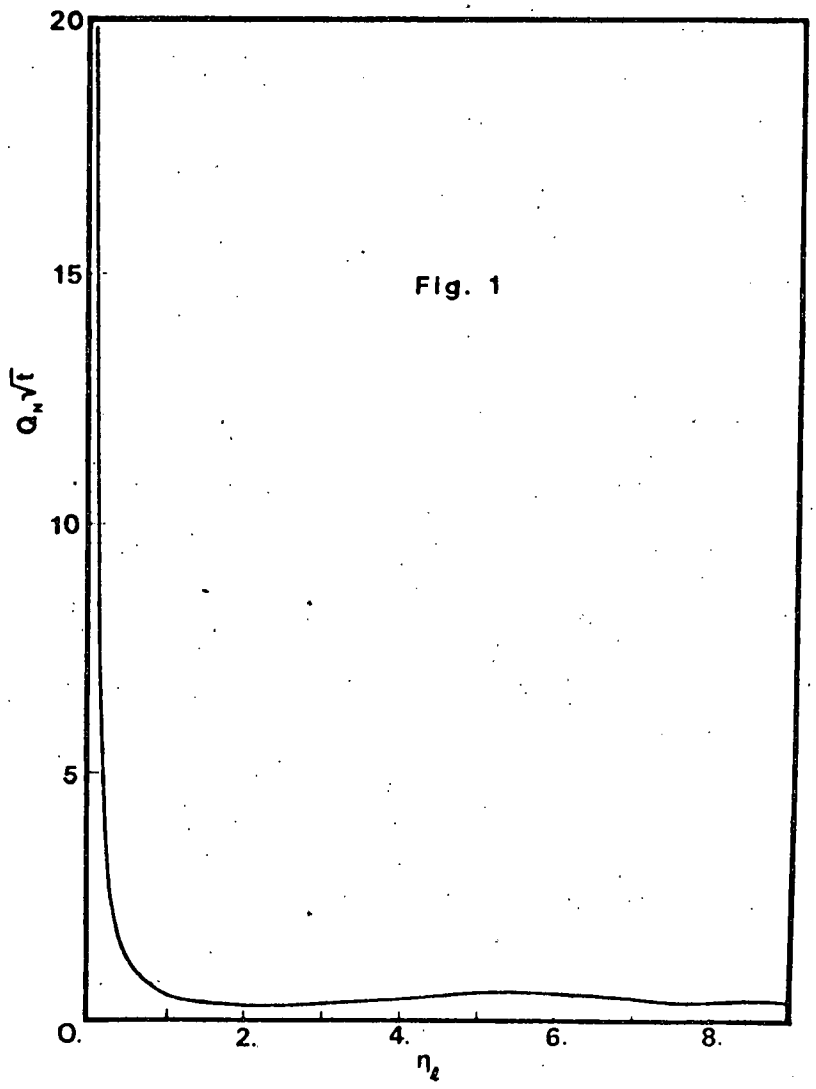

Fig. 1

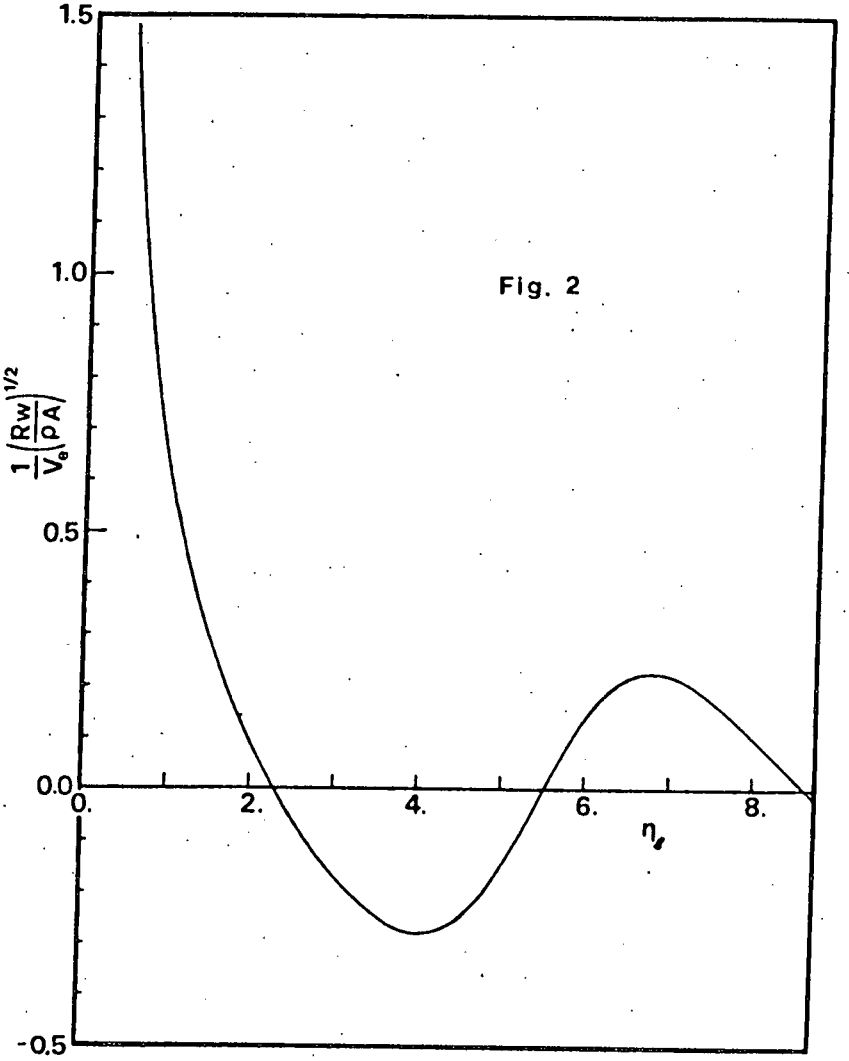

Fig. 2

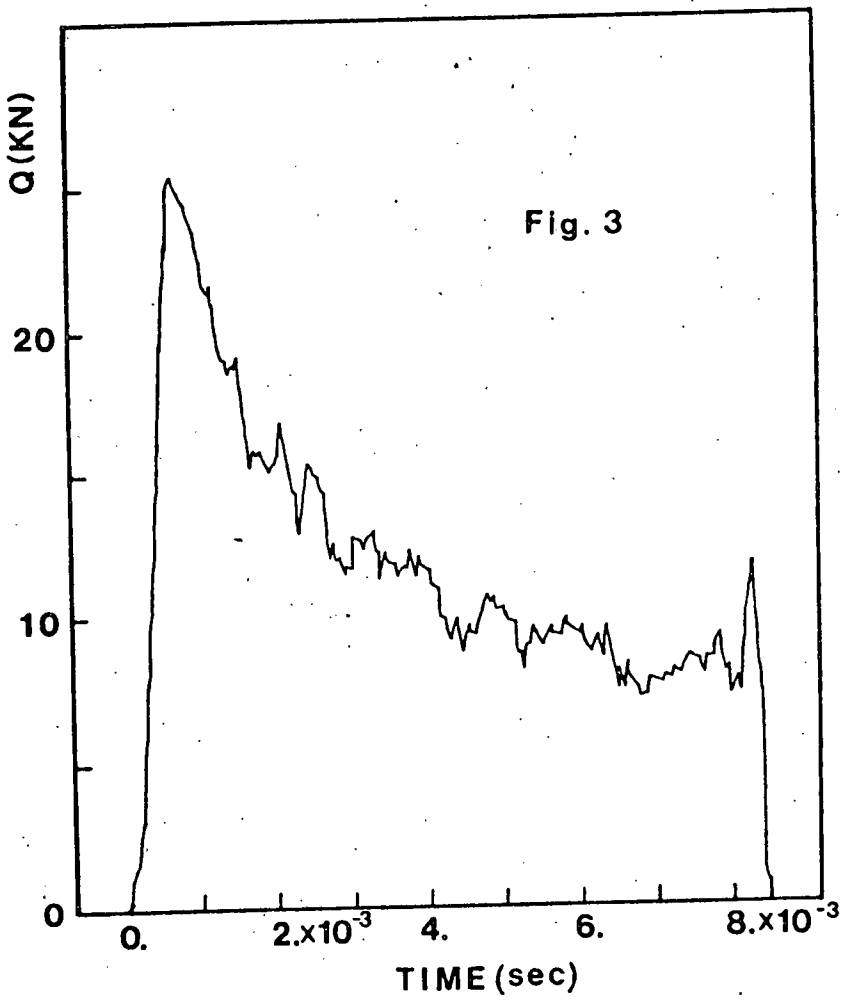

Fig. 3

Fig.4

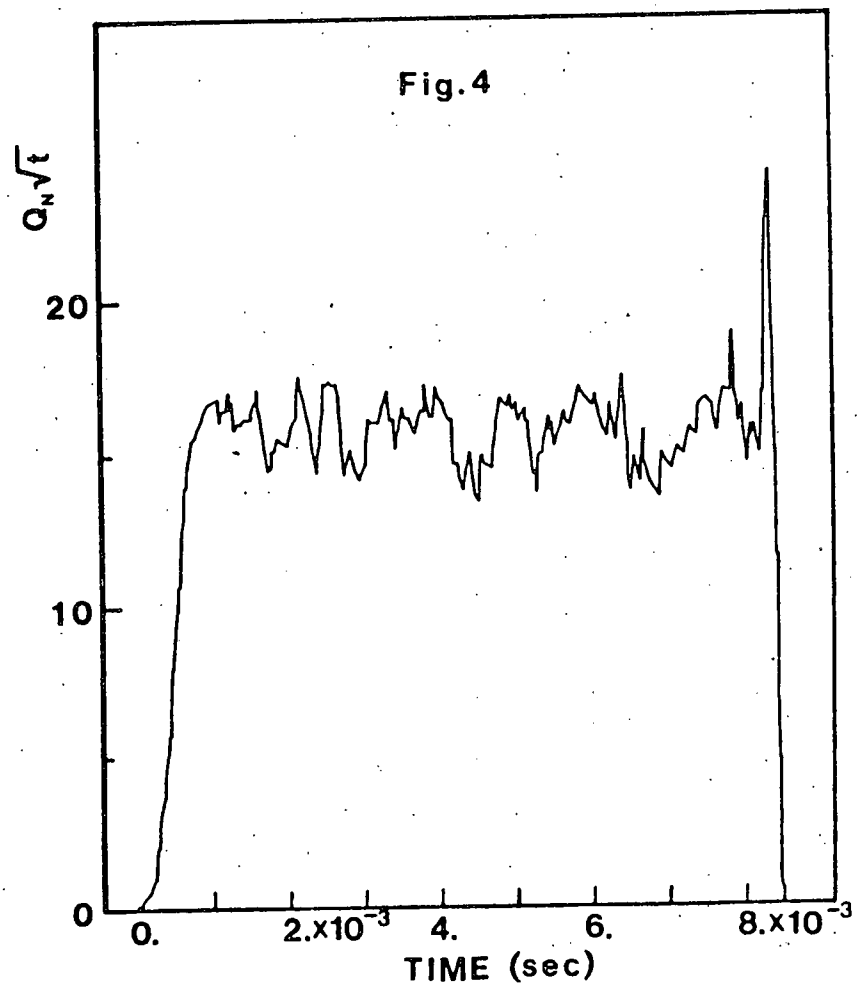

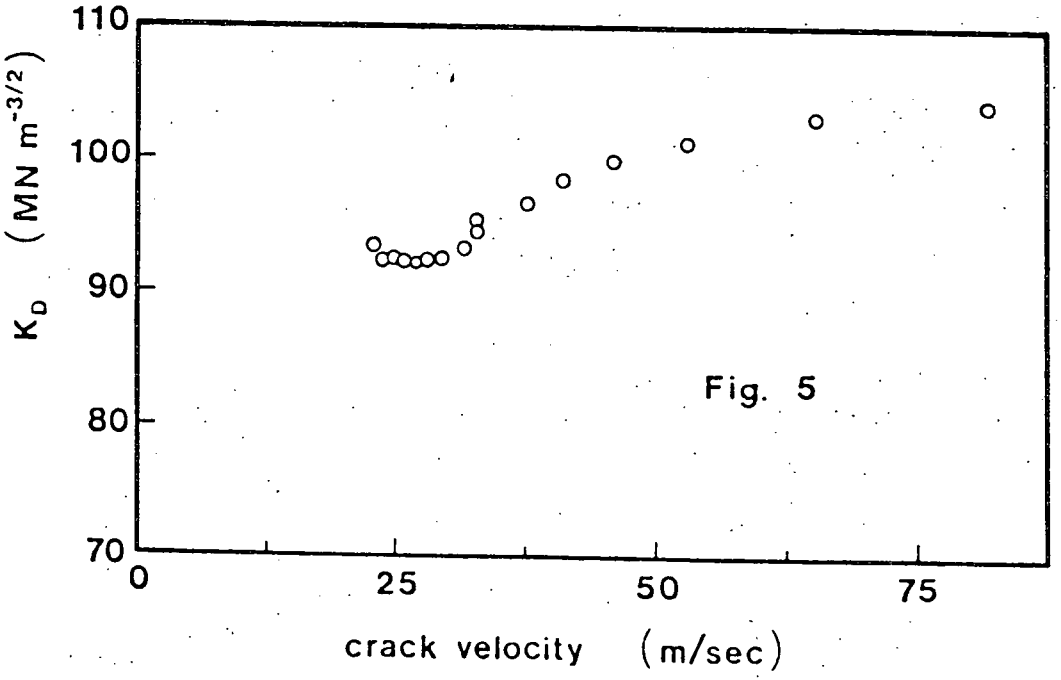

Fig. 5

Fig. 6

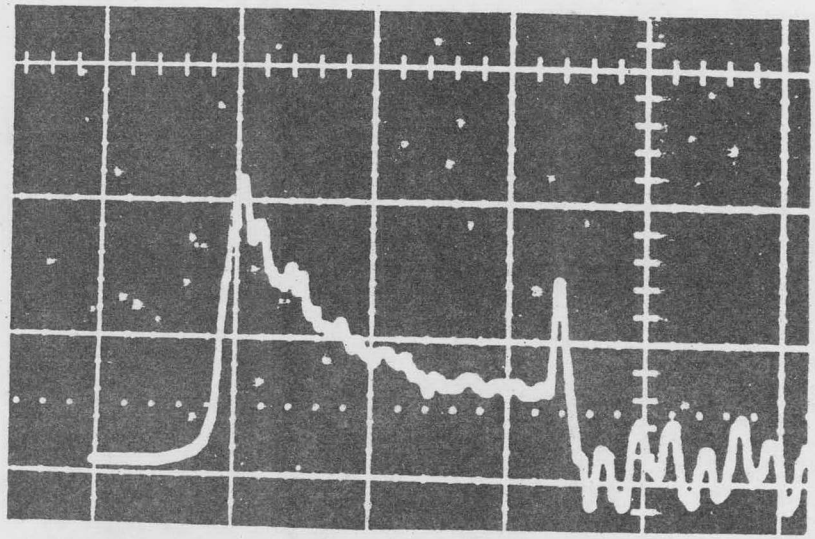

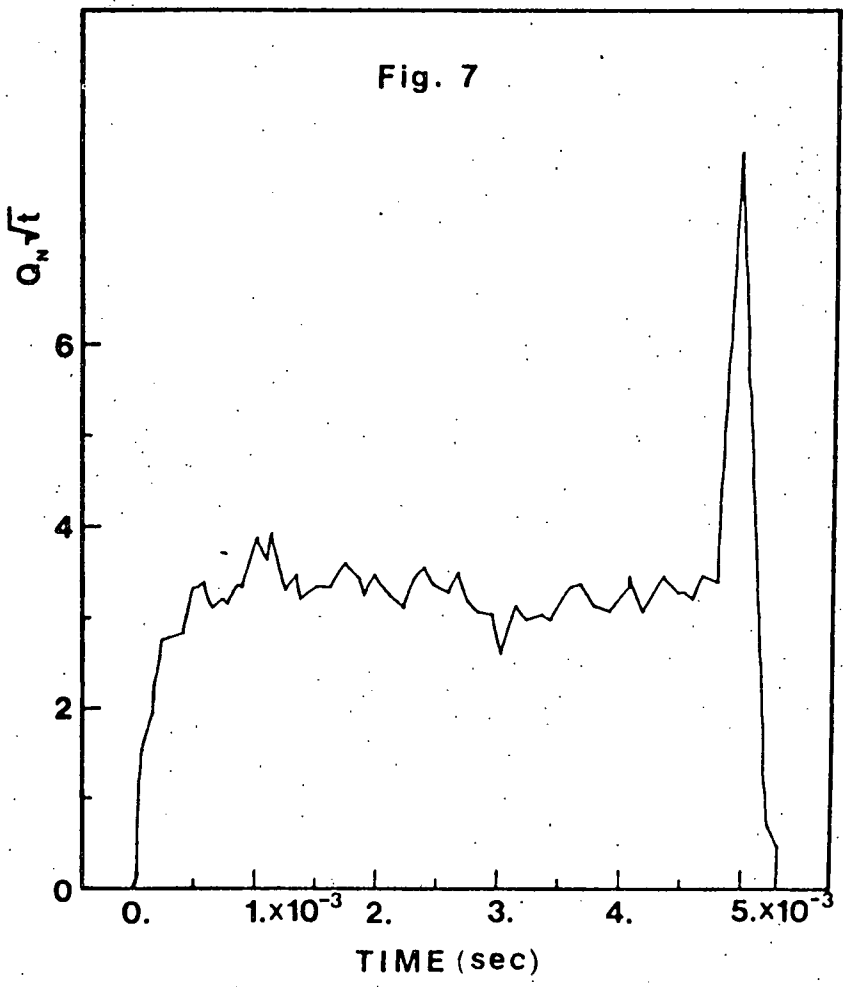

Fig. 7

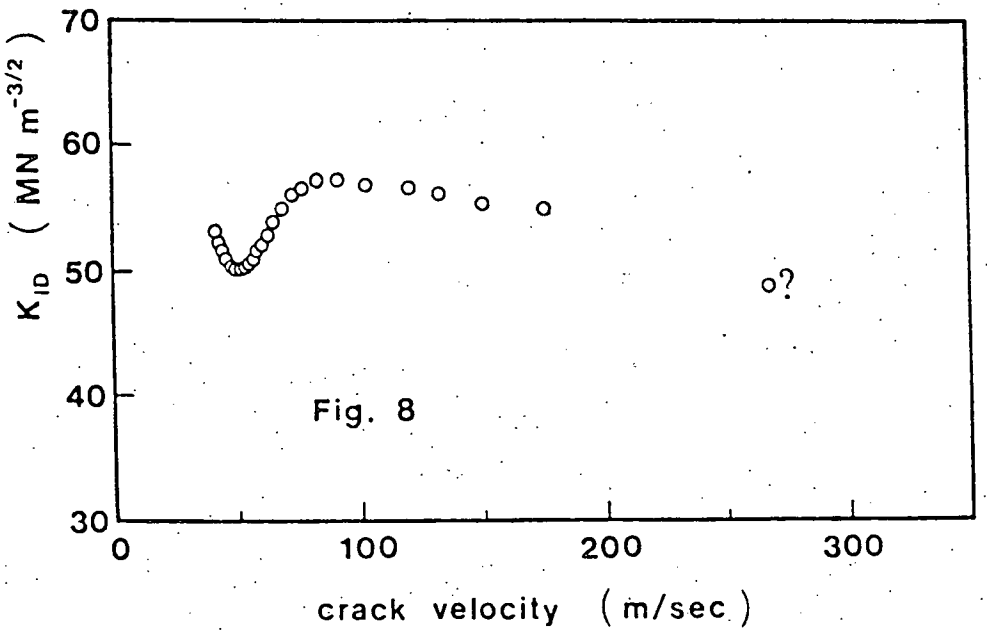

Fig. 8